THE VALUE OF PERFORMANCE.
NORTHROP GRUMMAN

Absolute and Relative Validation of ATMS Geolocation

Chunming Wang, Degui Gu, Alex Foo
Northrop Grumman Corporation, One Space Park, Redondo Beach, CA 90278

Technical Approach

The validation of the geographical registrations of the radiances measured by the Advanced Technology Microwave Sounder (ATMS) on board the Suomi NPP satellite can be achieved through comparison between these radiances with model predictions generated based on either a digital land mask or the accurately geo-located emissive band radiances of the Visible Infrared Imaging Radiometer Suite (VIIRS). The former is referred to as an absolute validation while the latter is referred to as a validation relative to VIIRS.

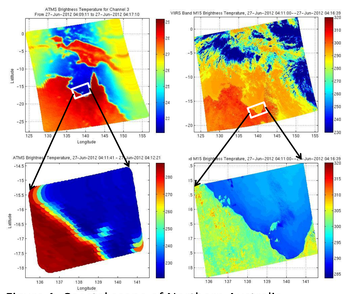

Figure 1. Coastal scene of Northern Australia

We have developed a systematic approach for estimating geolocation errors due to imperfect spacecraft or instrument alignments. Our approach makes use of the clear contrast in brightness temperature between ocean and land in coastal scenes illustrated in Figure 1. The example in Figure 1 also shows that the infrared and the microwave scene brightness are substantially different. In particular, coastal region in infrared scene can be obscured by cloud. A close examination of the distribution of the scene brightness for channel 3 of ATMS and M15 band of VIIRS, shown in Figure 2, reveals the expected bimodal distribution in both data, as well as, substantial difference in these distributions. In particular, the transition between the land and ocean brightness is much sharper for VIIRS because of the higher spatial resolution of the instrument. On the other hand, there is much wider spread in scene brightness for both land and ocean in the VIIRS data. Fundamentally our approach relies on the analysis of correlation between predicted scene brightness by averaging VIIRS data inside of each ATMS footprint, the differences in scene brightness may reduce the sensitivity of the correlation to misalignments. Using statistical analysis of the scene brightness as illustrated in Figure 2, we can identify a dividing threshold for land and ocean pixels. Using this threshold, a saturated high resolution coastal scene can be generated from VIIRS data as follows:

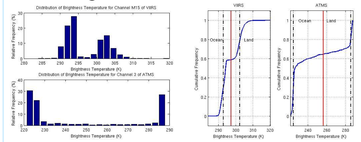

Figure 2. Distributions of scene brightness for ATMS and VIIRS

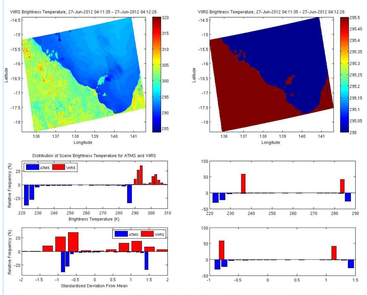

Figure 3. Brightness for original and saturated VIIRS scene

$$T_{Sat} = \begin{cases} T_{Ocean}, & T_{VIIRS} < R_{Ocean}; \\ T_{Ocean}\dfrac{T_{VIIRS} - R_{Land}}{R_{Ocean} - R_{Land}} + T_{Land}\dfrac{R_{Ocean} - T_{VIIRS}}{R_{Ocean} - R_{Land}}, & R_{Ocean} \le T_{VIIRS} \le R_{Land}; \\ T_{Land}, & T_{VIIRS} > R_{Land}, \end{cases}$$

where R_{Ocean} and R_{Land} represent the upper threshold for ocean scene brightness and the lower threshold for land scene brightness, respectively. On the other hand, T_{Ocean} *and* T_{Land} are selected brightness to represent land and ocean microwave scenes. An example of the saturated VIIRS data is shown in Figure 3. At a first glance, the saturated scene looks like a land mask. Indeed, when a digital land mask is used in simulation of the ATMS brightness, we can simply assign a brightness of T_{Ocean} *or* T_{Land} to a pixel in a digital land mask according its surface type.

The key step in our validation approach is to simulate the brightness temperature ATMS should be measuring based on high resolution scene brightness. The simulated brightness is a weighted average of the scene brightness inside the footprint of an ATMS Field of Regard (FOR). The weighting of each high resolution pixel depends on angular coordinates of its view vector in the ATMS's Focal Plane Array (FPA) frame and the antenna gain of the instrument in the direction of the view vector. The computation of the view vector relative to the ATMS FPA associated with each high resolution pixel is exactly the reverse process of the geolocation in the Sensor Data Record (SDR) generation code. All information necessary for the geometric transformations in this reverse process are provided in the SDR products for ATMS and VIIRS. An example of a simulated ATMS brightness scene is shown in Figure 4. As shown in Figure 4(b) the footprints of ATMS FORs have substantial overlaps. It is indeed due to this oversampling that there is an opportunity to detect geolocation errors smaller than the nominal size of the ATMS footprints. On the other hand, when all simulated and actual ATMS brightness temperatures are arrayed according to the cross-track FOR number and the scan number, we obtain an rectangular array of pixels in the *sensor space*. A measure of similarity between the simulated and the actual scene brightness is given by the cross correlation coefficient of the two images. It is not difficult to see from Figure 4 that the cross-correlation coefficient may be reduced by the difference in brightness variations of a microwave and a infrared scenes. Alternatively, we have developed an edge detection algorithm specifically trained to identify the transition points between ocean and land. The algorithm relies on

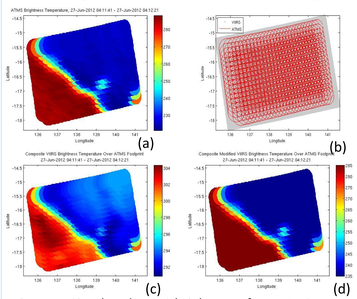

Figure 4. Simulated ATMS brightness from VIIRS M15 band radiances (c) and saturated radiances (d) in comparison with original ATMS data (a) and nominal ATMS footprints (b).

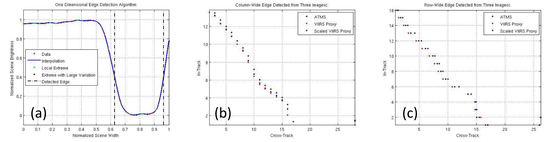

Figure 5. One dimensional edge detection algorithm (a) detects scene brightness variation exceeding a threshold between two local extreme data points. The column (b) and row direction (c) edges detected for Australia coastal scene are shown.

a one-dimensional edge detection approach where location of mid-scene brightness between two local extreme points with scene brightness variation exceeding a specified threshold is identified as an edge. This algorithm identifies a list of edges for each row and column of a picture. By comparing the locations of edges in two different images, we obtain a measure of how accurately the coastal lines are matched in these images.

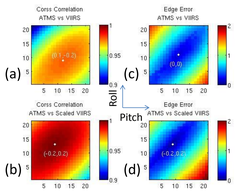

Figure 6. Alignment errors estimated by maxima of cross correlation coefficients between ATMS data and simulation using VIIRS (a) and saturated VIIRS (b) data, aw well as, the minima of edge errors compared to VIIRS (c) and saturated VIIRS (d) data.

In summary, we developed 4 measures of goodness of coastal line matching for each pair of ATMS and VIIRS scenes. These are the cross correlation coefficient between the ATMS data and the simulated ATMS scene using VIIRS or saturated VIIRS images and the differences in row and column edges in those images compared to the actual ATMS data. The estimation of the alignment error is obtained by incrementally varying the attitude biases of the instrument used in the generation of simulated ATMS scene brightness and finding the attitude biases that leads to either the maximum in the cross correlation coefficients or the minimum in the edge location errors. Figure 6 shows an example of the changes of the 4 measures of scene brightness matching as a function of pitch and roll alignment biases. As to be expected, we can see that the measures of mismatch is much more sensitive to alignment error for the saturated VIIRS data than the VIIRS data. In the case shown in Figure 6, the estimates for the alignment biases from the cross correlation and those from edge location error are also more consistent for the saturated VIIRS data than those obtained using the VIIRS data.

Validation Results

We have applied the approach described above to 4 manually selected scenes, shown in Figure 7, from June 27, 2012 with minimum cloud intrusion. The estimates for alignment biases for these 4 cases show significant consistency. These results, see Table 1 indicate that the ATMS geolocation has a -0.2 degree of pitch bias and a 0.15 degree of roll bias relative to VIIRS. These results are also consistent with results obtained by other teams. We have also examined the changes in the edge locations errors and the brightness temperature differences before and after the application of attitude bias correction. As shown in Figure 8, both type of errors are reduced significantly.

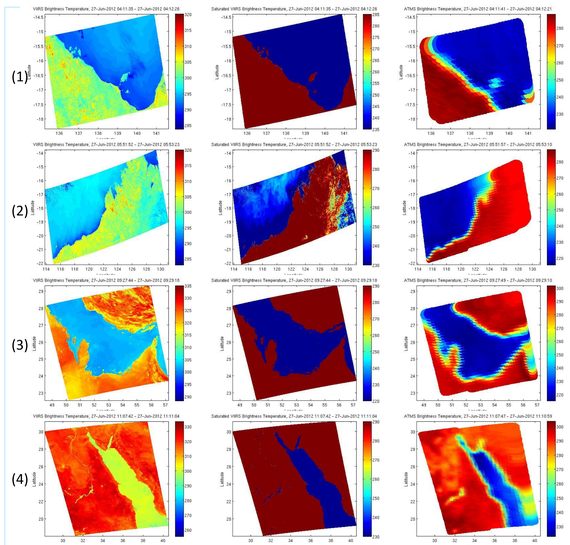

Figure 7. Four selected scenes from June 27, 2012 used in the ATMS geolocation validation

	Pitch (deg)	Roll (deg)
1	-0.2	0.2
2	-0.1	0.1
3	-0.2	0.1
4	-0.3	0.2
Ave	-0.2	0.15

Table 1. Estimates of alignment biases

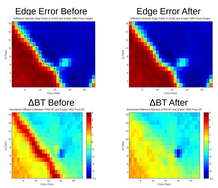

Figure 8. Changes in edge location and brightness temperature errors before and after optimal alignment biases are applied

Conclusion

The geolocation validation approach presented here provides an effective way to estimate geolocation errors due to instrument or satellite alignment biases. This method is sufficiently sensitive to enable detection of alignment biases much smaller than the nominal footprint size of the instrument. When used with a high resolution digital land mask, this approach has the potential to be used in an automated and systematic geolocation validation tool for a microwave instrument.